Fuel 346 (2023) 128314

Contents lists available at ScienceDirect

Fuel

journal homepage: www.elsevier.com/locate/fuel

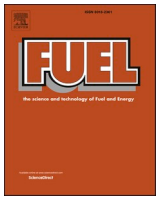

Binary mixtures of biomass and inert components in fluidized beds: Experimental and neural network exploration

Vincenzo Del Duca [a], Paola Brachi [a,*], Riccardo Chirone [a], Roberto Chirone [b], Antonio Coppola [a,*], Michele Miccio [c], Giovanna Ruoppolo [a]

[a] Istituto di Scienze e Tecnologie per l'Energia e la Mobilità Sostenibili, Consiglio Nazionale delle Ricerche, P.le V. Tecchio, 80-80125 Napoli, Italy
[b] Dipartimento di Ingegneria Chimica, dei Materiali e della Produzione Industriale (DICMaPI) Università degli Studi di Napoli Federico II, Piazzale V. Tecchio 80, 80125 Napoli, Italy
[c] Dipartimento di Ingegneria Industriale (DIIN), Università degli Studi di Salerno, via Giovanni Paolo II 132, 84084 Fisciano, SA, Italy

ARTICLE INFO

Keywords:
Fluidization
Binary mixtures
Artificial neural network
Segregation
Mixing
Canonical Correlation Analysis

ABSTRACT

In light of the little understanding of the hydrodynamics of multicomponent particle beds involving biomass, a detailed investigation has been performed, which combines well-known experimental and theoretical approaches, relying, respectively, on conventional pressure drop methods and artificial neural network (ANN) techniques. Specific research tasks related to this research includes: i. to experimentally investigate by means of visual observation the mixing and segregation behavior of selected binary mixtures by varying the biomass size and shape as well as the properties (size and density) of the granular solids in cold flow experiments; ii. to carry out a systematic experimental investigation on the effect of the biomass weight and volume fractions on the characteristic velocities (i.e., complete fluidization velocities and minimum slugging velocity) of the investigated binary mixtures in order to select the critical weight fraction of biomass in the mixtures beyond which the fluidization properties deteriorate (e.g., channelling, segregation, slugging); iii. to analyze the results obtained in about 80 cold flow experiments by means of ANN techniques in order to scrutinize the key factors that influence the behavior and the characteristic properties of binary mixtures. Experimental results suggest that the bed components' density difference prevails over the size difference in determining the mixing/segregation behavior of binary fluidized bed, whereas the velocities of minimum and complete fluidization increased with the increase of the biomass weight fraction in the bed. The training of ANNs demonstrated good performances for both outputs (U_{mf} and U_{cf}), in particular, best predictions have been obtained for U_{mf} with a MAPE $< 4\%$ ($R^2 = 0.98$), while for U_{cf} the best ANN returned a MAPE of about 7% ($R^2 = 0.93$). The analysis on the importance of single input on ANN predictions confirms the importance of particle density of the bed components. However, unexpected results showed that morphological features of biomass have a limited importance on U_{cf}.

1. Introduction

Several unique operational advantages, like fuel flexibility, uniform temperatures, intense solids mixing and efficient heat transfer, have made the fluidized beds the most efficient and widely applied reactors for the conversion of biomass into useful forms of bioenergy and/or biofuels.

Gas fluidized beds with poly-dispersed particles of different sizes, densities, and shapes are encountered in many industrial processes aiming at the production of energy, material and resources for greenhouse emissions mitigation and renewable resources utilization [1]. Design and operation of such systems deeply rely on the estimate of the minimum fluidization velocity (U_{mf}) of the mixture in order to maximize particle mixing and avoid undesired channeling and segregation. Many correlations have been developed so far in the pertinent literature to predict the U_{mf} of poly-dispersed binary mixtures containing biomass particles, [2–4], but these still exhibit considerable limitations in terms of accuracy and/or applicability, turning out system-specific, as highlighted in more recent literature reviews on the topic [5,6].

The development of experimental models based on physicochemical relations are, however, expensive in terms of time and money.

In this framework, artificial intelligence, and in particular machine

* Corresponding authors.
E-mail addresses: paola.brachi@stems.cnr.it (P. Brachi), antonio.coppola@stems.cnr.it (A. Coppola).

https://doi.org/10.1016/j.fuel.2023.128314
Received 9 November 2022; Received in revised form 22 March 2023; Accepted 3 April 2023
Available online 19 April 2023

learning (ML) techniques, has the potential to overcome the limitations of first principles models, as it can learn complex behaviors from dataset with a low-cost development of the model.

The main advantage related to the application of ML techniques is that definition of a prior model is not required because it is possible to build predictive models – also with limited cognition of the problem – mining data's inherent related information.

Among several ML techniques, artificial neural networks (ANNs) are extensively used in different fields such as machine diagnostics, pattern recognition, quality control as well as fitting experimental data, gaining in the years a relevant role also in chemical engineering [7].

Also in the field of multiphase systems, the scientific community implemented different ML techniques to solve problems related to the prediction of specific parameters and how the material properties, the operating conditions and the equipment features influence these latter [8–17]. In this regards, Chew & Cocco [8,9] tried to use ML techniques (random forest (RF) and ANN) to understand and predict the hitherto not fully understood fluidization phenomena in circulating fluidized bed (CFB) systems. They used RF to investigate the relative influence of the process variables (material type and operating conditions) on the local mass flux, concentration, segregation, and cluster characteristics. The results revealed how some variables are mainly influenced by geometric characteristics of the CFB systems, others strongly depend on operating conditions while still others, which are more or less equally influenced by all process variables. Conversely, the ANN was trained to predict the output variables giving back good prediction for some output with a mean NRMSE value of about 0.04 and R^2 values above 0.9; for other output variables the ANN gave poor prediction, probably due to the lack of accounting of some reactor characteristics. Despite this missing information, the authors improved the poor prediction trainings with a more accurate choice/elimination of the input variables based on the ranking of importance by the RF method. ANN was also used by Fu et al. [10] to predict the macroscopic flow characteristics of particles in a bubbling fluidized bed, as function of particle properties, gas velocity, gas distributor, axial position and radial position. The ANN training shows that the flow characteristics are affected by several factors with the following importance rank Axial position > Radial position > Gas properties > Gas distributor. Moreover, the results obtained from ANN were compared with theoretical calculations based on constitutive equations, which have been less accurate than ML technique. Instead, Perazzini et al. [17] tested the ability of ANN to estimate drying kinetics in fixed, fluidized and vibro-fluidized bed dryers under different operating conditions. The results show that the model is able to estimate new patterns just for the cases in which the database refers to a single type of dryer. Conversely, the developed networks showed difficulty to learn multiple patterns from different type of dryers, resulting in predictions with low accuracy, because information in the dataset about the different gas–solid contact were not present. This demonstrates the importance to choose proper input variables in the dataset for an efficient prediction. As concern the prediction of the minimum fluidization velocity (U_{mf}), several authors used different ML techniques with a preponderance of ANNs. Targino and coworkers [14] trained ANN to evaluate the key factors that influence the condition of minimum fluidization of acai berry residues. The performances of trained ANN have been encouraging, because able to predict in a quite fairly good way the minimum fluidization velocity for conditions not present in the original dataset, demonstrating the potentialities of the ANN. It is worth to cite the work of Zhou and colleagues [15], because they combine the application of ANNs for U_{mf} with a text mining approach for the automatic creation of the dataset. The text mining analyzed about 40,000 papers and the result was a dataset formed by more than 1400 observations, which include particle and fluid characteristics and operating conditions. The predictions of the ANN offer a better capability to estimate U_{mf} with respect to Ergun and Wen − Yu correlation. Other authors focused their attention on the evaluation of the U_{mf} in spouting beds [12,13] concluding that the ANNs provide reliable predictions, better than empirical correlations. Rushd et al. [11] compared different ML techniques used singularly or in combinations for the estimation of the terminal settling velocity of spherical and non-spherical particles in Newtonian and non-Newtonian fluid. In particular, the results highlighted that the RF regression model provided the best performance compared the other models used singularly, while the combination of different ML techniques performed very similar to the RF model but showed a more elevated computational complexity.

In an attempt to develop more accurate and generic correlations and to provide additional insight on predicting the fluidization behavior of biomass-based binary mixtures, an experimental investigation aiming at analyzing the fluidization behavior of highly poly-disperse binary mixtures consisting of small and dense inert particles mixed with less dense and coarse pieces of biomass fuels has been performed by using a borosilicate glass fluidization column (0.10 m ID) equipped with a 4-mm-thick sintered-glass gas distributor and the results are presented in this paper. Specifically, peels of fresh oranges, which mimic the solid by-products of orange fruit processing, and tomato peels, which are the by-product of the peeling of tomatoes used for canning, were used as the biomass component due to the increasingly interest they are gaining as a potential feedstock for bioenergy and biofuels productions [18,19]. Four different kinds of granular solids, consisting in both inert materials (i.e., Ticino sand and quartz sand) and catalysts (i.e., alumina powder and alumina spheres), were used as the main bed component in order to test the influence of either size or density on the mixing/segregation behavior as well as on the characteristic velocities of the investigated binary systems. Fluidization tests were performed at ambient temperature to prevent that the formation of endogenous bubbles from devolatilizing fuel particles could come into play, which also affects mixing and segregation phenomena in real fluidized bed reactors [20]. Experimental runs at different weight fraction of the biomass in the bed were carried out to investigate the impact of the bed composition on the characteristic velocities (i.e., the minimum fluidization velocities, U_{mf}, and the complete fluidization velocities, U_{cf}) of the considered binary systems as well as determine the critical value of the biomass weight fraction beyond which the quality of fluidization deteriorate (e.g., channelling, irreversible segregation, slugging). To complement this study, an ANN was developed in MatLab environment, using the experimental data, in order to create a predictive tool for U_{mf} and U_{cf} for binary mixtures composed by biomass and inert material. The set-up of ANN was optimized in terms of type of neural network, number of neutrons and training functions. The prediction performance of ANN was compared to the outcome of a model developed by the adoption of a multivariate statistical analysis named Canonical Correlation Analysis (CCA). Finally, for the best performing ANN, a specific analysis was carried out to discriminate the factors playing the greatest influence on the estimation of U_{mf} and U_{cf}.

2. Materials and methods

2.1. Feedstock sampling and preparation

Peels of fresh oranges, which mimic the solid by-product of orange fruit processing, and tomato peels, which are the residues arising from the peeling of tomatoes used for canning, have been used as the biomass components in this study. In more details, the peels of fresh oranges were separated from the pulp by hand, whereas the tomato skins were collected from a tomato processing industry in Salerno (40°47′24.5″N, 14°46′15.8″E), in the Campania region of Italy (IT). Both the raw biomass samples were subjected to preliminary operations of drying and size-reduction. In more details, raw peels of orange (74.7 %wt. moisture content) and tomato (80.5 %wt. moisture content) were conditioned down to a moisture content of about 6–8 %wt., which represents the equilibrium values that the materials reached when left in a laboratory fume hood at room temperature for about 48 h. After drying, both the feedstocks were ground in a batch knife mill GM 300 by Retsch for 10 s

at a speed of about 3000 rpm and the 1–2 mm sieve fraction was retained for the subsequent fluidization tests (hereafter referred to as fine tomato peels (FTP) and fine orange peels (FOP). Fig. 1 shows the images of both the samples so as they were fed to the fluidized bed reactor. Five types of granular solids were selected in this work as the bed material to assist the biomass fluidization, namely: 1. fine quartz sand in the size range of 100–250 μm (FS); 2. coarse silica (Ticino) sand in the size range of 150–400 μm (CS); 3. fine commercial γ-alumina powder (PURALOX SCCA-150/200, SASOL) in the size range of 50–250 μm (FA); 4. ultra-fine commercial γ-alumina powder (obtained as a sieving fraction of PURALOX SCCA-150/200, SASOL) in the size range of 63–180 μm (UFA); and 5. coarse commercial γ-alumina spheres (PURALOX alumina spheres 0.3/180, SASOL) in the size range of 200–400 μm (CA). Binary mixtures under study will be coded below as follows: X/Y-Z where "X" stands for the inorganic bed component, "Y" is the abbreviation of the biomass feedstock name and "Z" stands for the weight fraction of the biomass in the bed.

2.2. Particle characterization

The particle-size distribution of the investigated materials was determined by using a laser diffraction analyzer (Mastersizer 2000, Malvern Instrument Inc.), with an analytical size range of 0.2–2000 μm. Granular solids were characterized by means of the Sauter mean diameter D[3,2], which represents the quantity typically adopted to describe mean size of a given particle distribution in the case of interphase processes (such as drag forces or heat exchange), in which the specific surface area plays a major role. Five replicate measurements were performed for each sample and the obtained D[3,2] values are shown in Table 1 as the mean value of the data provided by the Malvern Mastersizer 2000 software. A helium gas pycnometer (Quantachrome Ultrapycnometer 1000) was used to determine the skeletal density (ρ_S) or the true density of both biomass and inorganic compounds. Experimental runs were carried out on samples oven dried at 105 ± 5 °C for 24 h. Five replicate measurements were performed for each sample and the ρ_S-values are shown in Table 1 as the mean value of the obtained data.

Nitrogen adsorption and desorption tests were also carried out at −196 °C using a Quantachrome Autosorb 1-C instrument, which allowed determining the total pore volume (PV, cc/g) of the samples under study. Both the obtained skeletal density and pore volume data were then adopted to estimate the envelope particle density (ρ_P), which is typically determined for porous materials when pore spaces within material are included in the volume measurement of samples, by means of the following Eq. (1):

$$\rho_P = \frac{\rho_S}{1 + PV \bullet \rho_S} \tag{1}$$

where ρ_S and PV are respectively expressed in g/cm^3 and cm^3/g. Loose (ρ_{lb}) and packed (ρ_{tb}) bulk densities of bed components were finally determined through standard techniques, i.e., by using sample weight and volume, with the latter also including the contribution of the inter-particle void volume. In more detail, the bulk density was determined as the mass to the volume ratio of a sample poured into a graduated cylinder without compacting. When measuring the packed density, instead, a step of material compaction was included. Table 1 also summarizes the properties of bed compounds used in a previous study of the Authors [21], whose obtained data have also been included in the statistical and neutral network analyses performed in this work.

2.3. Experimental setup and cold fluidization test procedures

Fluidization tests at ambient temperature were carried out using a cylindrical column (100 mm inner diameter and 750 mm height) made up of clear borosilicate glass, which allows the visual observation of the fluidization pattern and movement of particles in the bed during the experimental runs. A 6-mm-thick sintered-glass gas distributor disk (nominal pore size of 16 – 40 μm) located at the bottom of the column supported the bed materials and ensured a uniform distribution of the fluidizing gas. The pressure acquisition system was composed of two piezoresistive pressure sensors (GE Druck PTX 7200 Series Pressure Transmitter with a working pressure range from 0 to 250 mbar) connected to a USB data acquisition device (Pico USB TC-08) and located the first one just a few centimeters above the distributor plate, the second one in the freeboard. Fluidization experiments were performed at room temperature in order to prevent that the formation of endogenous bubbles from devolatizing fuel particles could come into play, which also impacts mixing and segregation phenomena in real fluidized bed reactors [21]. A schematic sketch of the adopted lab-scale fluidized bed reactor is shown in Fig. 2. Fluidization tests were carried out on beds consisting of either only inorganic (inert or catalytic) particles or binary mixtures obtained mixing pre-set amounts of biomass and dense granular solids, while keeping the bed aspect ratio nearly constant (i.e., H/D ≈ 2.2 ± 0.2).

Even though most studies in the literature focus primarily on beds with aspect ratios equal to or less than unity, typically described as

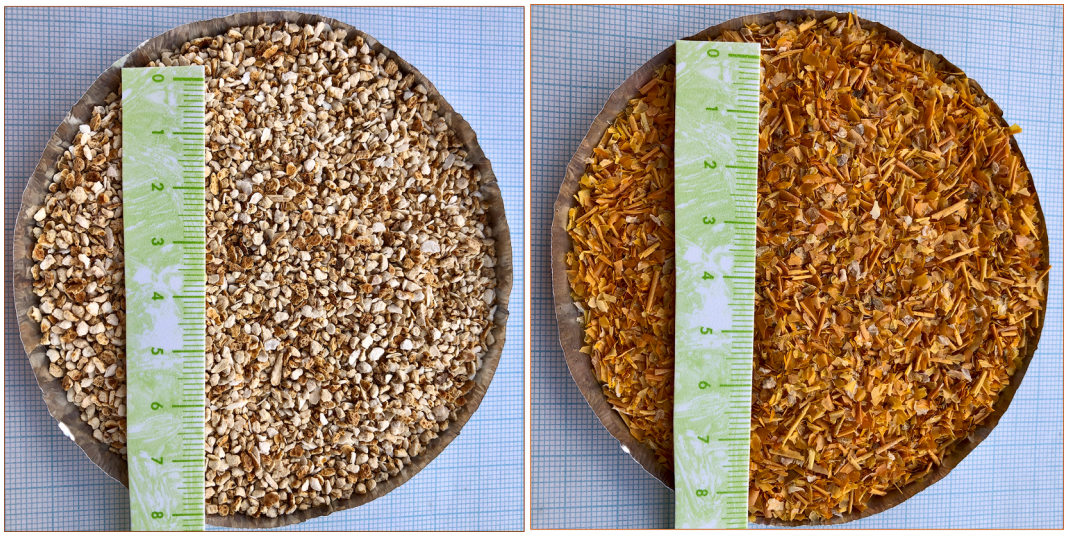

Fig. 1. Pictures of the orange (left side) and tomato (right side) peels samples used in the cold fluidization tests. (For interpretation of the references to colour in this figure legend, the reader is referred to the web version of this article.)

Table 1
Properties of biomass and inert particles used in this study.

	Fine Quarz Sand **FS**	Coarse Silica Sand **CS**	Ultrafine Al_2O_3 Powder **UFA**	Fine Al_2O_3 Powder **FA**	Coarse Al_2O_3 Spheres **CA**	Fine Orange Peels **FOP**	Coarse orange peels **COP**	Fine TomatoPeels **FTP**
Size range, μm	100–250	150–400	63–180	50–250	200–400	1000–2000	5000x5000 (OP slabs)	1000–2000
D[3,2], μm	139.8	209.9	92.4	123.7	286.1	–	–	–
ρ_s, kg/m^3	2813.5	2650.6	3986.9	3986.9	3986.9	671.7	671.7	1049.9
ρ_p, kg/m^3	2813.5	2650.6	1250.3	1250.3	1479.7	469.4	421.1	745.8
ρ_{lb}, kg/m^3	1444.7	1367.1	758.0	761.1	823.2	380.5	230.2	70.8
ρ_{pb}, kg/m^3	1575.0	1537.1	809.3	824.1	870.1	387.1	273.9	104.7
PV, cc/g	0	0	0.549	0.549	0.425	0.642	0.886	0.388
Geldart class	B	B	A	A	B	D	D	D

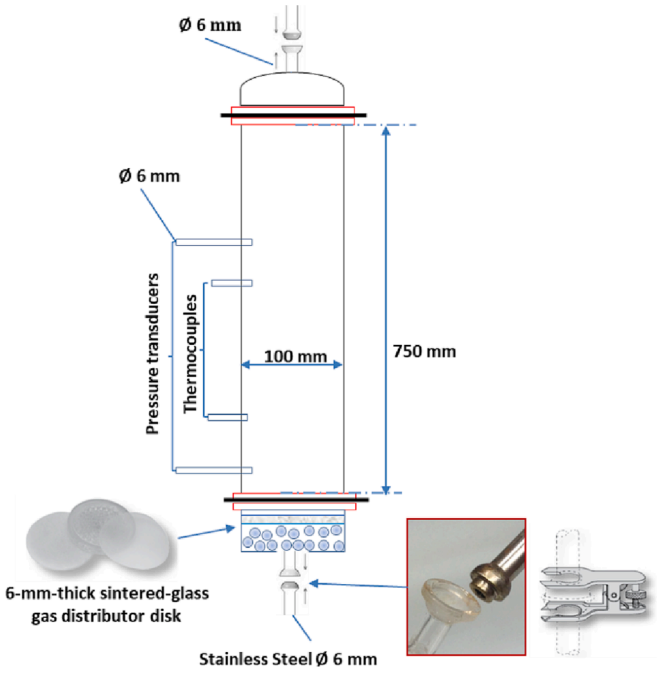

Fig. 2. Schematic of the lab-scale fluidized bed reactor used to perform cold fluidization tests of polydispersed binary mixtures including biomass particles.

shallow beds, the industrial application of bubbling fluidized bed reactors covers a wide range of aspect ratios. Deep bubble fluidized beds (i.e., bed with aspect ratio greater than 2), in particular, have certain advantages, including the more vigorous solids circulation and the increased reactant contact time, while ensuring uniform temperature and material distribution that make them very attractive for industrial applications [22]. Among these, in particular, it is believed that the more vigorous solid circulation that characterizes the deep fluidized beds compared to the shallow ones, could make the former particularly suitable for the treatment of poly-dispersed binary mixture including irregular particles of biomass, which have a marked tendency to segregate upon fluidization [21]. An aspect ratio in the order of 2.2 was, therefore, adopted in the present study, as it was assumed that such a value could be sufficiently high to ensure a more vigorous solid circulation, so as to minimize the onset of segregation phenomena, but at same time not so high to favor the occurrence of undesired slug phenomena that are very common in deep beds on a laboratory scale.

The evaluation of the characteristic velocity of binary mixtures has been a controversial subject in recent years [23]. Although, the fluidization of binary beds was traditionally analyzed by defining a minimum fluidization velocity, U_{mf}, to be determined (as done with any "mono-solid" systems) at the intersection between the (extrapolated) pressure drop line of fixed bed and the (extrapolated) horizontal line representing the suspended state, there is currently no a general agreement on its exact definition [23,24]. This is essentially a consequence of the fact that, as suggested by the actual phenomenology of the process, analysed in detail elsewhere [23–25], the onset of fluidization in a binary bed is a rather gradual process. Specifically, it occurs within a quite wide velocity range where the transient and partial fluidization of the bed is commonly accompanied by a complex sequence of mixing and segregation phenomena whose specific pattern depend on the properties of the binary mixture (i.e., the composition as well as difference in the size, the density and the shape of the bed components) as well as the initial arrangement of the fixed bed [26,27].

The peculiarities of this mechanism are fully reflected by the experimental pressure drop diagram of binary mixtures where two characteristic velocity thresholds can be typically recognized, just as shown in Fig. 3.A) for the specific case of a binary mixture obtained by the complete mixing of spheres differing only in diameter. These are the "initial fluidization velocity", U_{if}, at which ΔP first deviates from the fixed bed curve, and the "complete fluidization velocity", U_{cf}, at which the ultimate value of ΔP is first attained. Accordingly, some authors [23,28] have recently proposed the replacement of the conventional concept of minimum fluidization velocity, U_{mf}, as discussed above, with the new concept of complete fluidization state, whose corresponding velocity, U_{cf}, was defined as the superficial gas velocity where the bed pressure drop begins to deviate from the constant bed pressure line during defluidization. In line with the abovementioned arguments, during each experimental run the pressure drop across the bed was continuously recorded and the fluidization curves drawn in order to define the onset of both the conditions of incipient (U_{mf}) and complete fluidization (U_{cf}) by means of the conventional graphical methods. Specifically, U_{mf} was identified with the superficial gas velocity at the intersection of the pressure drop line corresponding to the state of fixed bed with the constant pressure drop line corresponding to the fluidization state [29], whereas U_{cf} was instead identified with the minimum value of the superficial gas velocity where a pressure drop equal to the weight of the bed per unit cross-sectional area is detected in the fluidization curve [21]. Finally, visual observation was used to identify the onset of the undesired slugging and segregation phenomena. The values of the U_{mf} and the U_{cf} were measured upon decreasing the fluidization gas flow rate to avoid dependence on the initial bed configuration. Hence, during each experiment, starting from the above-mentioned well-mixed regime, the airflow rate was gradually decreased to zero and the pressure drop across the bed continuously recorded. For each of the investigated binary mixtures (e.g., UFA/FOP, FA/FOP, FS/FTP and CS/FTP) several fluidization tests were performed by increasing the biomass weight fraction (X_B) into the bed; this approach made possible to both study the effect of the bed content on the characteristic velocities of the binary systems under study (i.e., minimum and complete fluidization velocities) and determine the critical value of X_B (i.e., the so called maximum biomass batch loading) beyond which the fluidization pattern deteriorates (e.g., channeling, segregation, slugging). As for fluidization tests relating to binary mixtures, the initial arrangement of

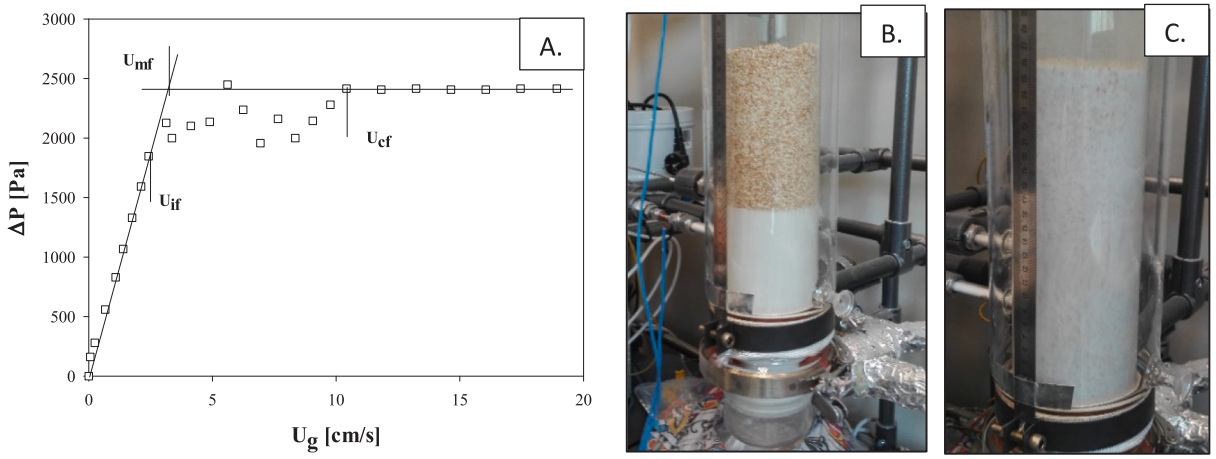

Fig. 3. A) Pressure drop diagram of a two component mixture obtained by the complete mixing of spheres differing only in diameter (adapted from [26]); B.) snapshot of the initial arrangement of the bed during the cold flow fluidization test performed on the CA/FOP-22 binary mixture: C.) snapshot of the CA/FOP-22 binary mixture frozen in a perfectly mixed condition by instantly bringing the fluidization gas flow to zero.

the bed was that with the bed components completely segregated and the biomass particles on the top (see Fig. 3. B). Starting from this fixed bed configuration, first the airflow rate was quickly set at 1500 Nl/h (corresponding to a superficial gas velocity of about 5 cm/s) and then gradually increased until a slugging or turbulent regime was observed. In most of the performed experimental runs, an air flow rate in the order of 1500 Nl/h proved to be sufficient to ensure a gradual transition (in<2 min) from the initial fully segregated fixed bed configuration (Fig. 3. B) to a well-mixed regime (Fig. 3. C) characterized by a uniform distribution of particles in the bed, as showed by the snapshots in Fig. 3, which refers to CA/FOP-22 binary mixture. However, in general, both the critical air flow rate and time required to reach a well-mixed regime slightly increased by increasing the biomass weight fraction in the bed for each of the investigated binary mixtures [21]. It is worth noting that if a too high initial air flow rate was adopted, the system exhibited an almost plug-flow behavior, which means that all particles were transported out of the bed with little back-mixing. In more details, in this work, the maximum biomass batch loading for the investigated binary mixtures was assumed equal to the biomass weight fraction value (X_B) beyond which, starting from a fully segregate fixed bed configuration, the further increase of the air flow rate above 1500 Nl/h did not result in a well-mixed regime but rather in a partially segregated bed with either residual biomass particles floating at the bed surface (flotsam) and exhibiting slugging regime or biomass particles sinking to the bottom of the bed (jetsam) as shown in detail in the Fig. 4, borrowed from a previous study of the authors [21].

To ensure the reliability of the experimental data, but without making the experimental campaign excessively time-consuming, only some tests (UFA/FOP-18; FA/COP-18; UFA/FOP-6; UFA/FOP-16; FA/FOP-16; FA/FOP-20; CA/FOP-18; CA/FOP-22) were randomly performed in duplicate, returning a relative error in the order of 3 and 2% on the determination of the minimum and complete fluidization velocity, respectively.

2.4. Canonical Correlation analysis and artificial neural networks

In a first phase, the parameters used as inputs were: inert material density $\rho_{particle}$ (kg/m^3), inert Sauter diameter d_{Sauter}, biomass volume fraction in the bed (%vol.), biomass characteristic size (i.e., prevailing length L_b, mm), biomass particle density $\rho_{particle}$ (kg/m^3), biomass sphericity factor Φ_b. In a subsequent phase, CCA inputs were linearly combined and incremented with the following ones: inert material bulk density ρ_{bulk} (kg/m^3), biomass bulk density ρ_{bulk} (kg/m^3), biomass weight fraction in the bed (%wt.). On the other side, the outputs parameters were: the minimum fluidization velocity U_{mf} and the complete fluidization velocity U_{cf}. As for the calculation of Φ_b, fine orange peels present a pseudo-spheroidal shape with relative proportions of 1:1:2 [30], so a value of 0.93 was set; for coarse orange peels and fine tomato peels the shapes resembled rectangular parallelepipeds with relative proportions of 1:4:4 and 1:2:4, so the values of Φ_b were set 0.64 and 0.68, respectively. L_b was defined as the average maximum dimension of the biomass particle; so, for fine orange peels, coarse orange peels and fine tomato peels L_b was 1.41, 5.00 and 1.04 mm, respectively.

These features were chosen on the base of the fact that from a practical point of view are simple to obtain for a biomass, and because are the typical features governing the Ergun's equation. In particular, L_b is considered as the characteristic size for the biomass, while bulk and particle densities are chosen as parameters which are correlated with void fraction ε. The feature related to fluidizing gas are not considered in the dataset because the air was used for all tests. The complete dataset – no missing data are present - has made available in the supplementary material.

The performance indicators are MAE, MSE, SAE, MAPE and R^2 calculated in the evaluation of the fluidization velocity but for simplification, only MAPE and R^2 have been reported here. Canonical Correlation Analysis (CCA) is widely used to extract the correlated patterns between two sets of variables. CCA looks at two sets of variables for modes of maximum correlation between the two sets. Thus, CCA sits at the top of a hierarchy of regression models where it is able to manage multiple predictors (inputs) and multiple predictands (outputs). If × is the set of predictors and y the predictands, then CCA can be used to predict y when new observations of × become available [31]. In this study, CCA is used as a starting and comparative statistical advanced analysis to the ANNs, in terms of performance (MAPE, R^2), relative to the minimum and complete fluidization velocity, U_{mf} and U_{cf}. In this study, ANNs were used to predict the minimum fluidization velocity U_{mf} and the complete fluidization velocity U_{cf}. Input and output parameters used are the same used for CCA analysis. Specifically, an algorithm, called "netoptim", was conceived within the present research and implemented in Matlab to develop a large number of ANNs, with the goal of evaluating different choices such as: i.) the network type (fitnet, feedforwardnet and cascadeforwardnet); ii.) the number of neurons in the hidden layer (set, initially, equal to the number of inputs ± 3); iii.) the training function. In this work, the Authors decided to set up the transfer function as an hyperbolic tangent sigmoid, in order to avoid a further parameter to investigate.

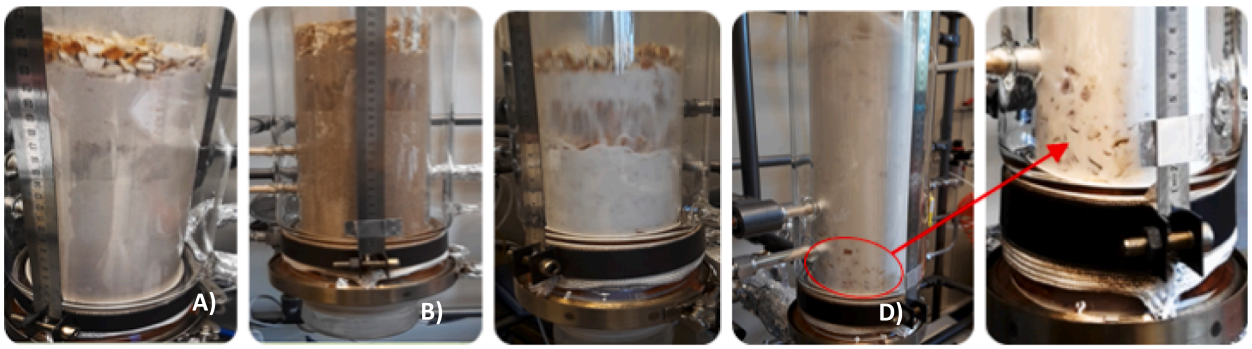

Fig. 4. Segregation and slug phenomena in: A) FS/COP-6 (X_B = 6.1 %wt.; 26.8 %vol.); B) CS/COP-7 (X_B = 7.1 %wt.; 24.6 %vol.); C) CA/COP-18 (X_B = 18.4 %wt.; 43.6 %vol.); and D) FA/COP-21 (X_B = 20.7 %wt.; 45.3 %vol.) binary mixtures at high fluidization number (U_g/U_{mf}) (Reproduced by permission from Brachi et al. [21]).

3. Results and discussion

3.1. Experimental results - dataset

Table 2 lists the values of the velocities of minimum and complete fluidization obtained for the investigated binary mixtures as borrowed from a previous study of the Authors [21].

3.2. Modelling results

Table 3 reports the results of the CCA analysis carried out for U_{mf} and U_{cf}, in terms of MAPE for different attempts (tests 1–5) considering different combinations of input variables.

Some inputs are fixed in all tests, such as the particle density of inert and biomass (ρ^I_{part} and ρ^B_{part}), the Sauter diameter of the inert (d^I_{Sauter}), the max average length (L_B) and the sphericity (Φ_B) of the biomass. Instead, the bulk density of inert and biomass (ρ^I_{bulk} and ρ^B_{bulk}) was considered only for tests 3 and 4, while the biomass fraction in the bed was reported

Table 2
Experimental operating variables and binary mixture characteristic velocities.

Binary mixtures	% wt. Biomass	%vol Biomass	U_{mf}, cm/s	U_{cf}, cm/s	Binary mixtures	% wt. Biomass	%vol Biomass	U_{mf}, cm/s	U_{cf}, cm/s
FS/COP-0	0	0.00	1.99	2.85	UFA/FOP-18	18.03	31.50	0.32	4.92
FS/COP-1	1.03	5.65	2.27	5.08	FA/FOP-0	0	0.00	0.68	2.04
FS/COP-2	2.04	10.69	2.35	5.62	FA/FOP-2	2.17	4.51	0.8	5.33
FS/COP-3	2.97	14.97	2.62	6.19	FA/FOP-4	4.1	8.34	0.73	5.33
FS/COP-4	4.18	20.05	3.17	6.63	FA/FOP-6	6.03	12.02	0.74	4.92
CS/COP-0	0	0.00	3.75	6.43	FA/FOP-8	8.03	15.67	0.74	4.92
CS/COP-1	1.04	5.57	4	5.24	FA/FOP-10	10.06	19.23	0.73	4.79
CS/COP-3	2.96	14.62	3.79	5.10	FA/FOP12	12.34	23.06	0.6	4.92
CS/COP-5	4.85	22.24	4.23	5.66	FA/FOP-14	14.16	25.99	0.66	4.92
FA/COP-0	0	0.00	0.68	2.04	FA/FOP-16	16.3	29.31	0.61	4.91
FA/COP-1	0.99	2.92	0.79	1.21	FA/FOP-18	18.18	32.11	0.55	5.31
FA/COP-3	2.91	8.27	0.76	1.72	FA/FOP-20	20.56	35.53	0.59	5.43
FA/COP-5	4.82	13.22	0.79	1.71	FA/FOP-22	22.07	37.61	0.57	5.68
FA/COP-7	6.61	17.56	0.77	2.04	FA/FOP-24	24.07	40.29	0.59	5.81
FA/COP-9	9.17	23.30	0.78	2.69	FA/FOP-26	26.27	43.13	0.6	6.60
FA/COP-11	10.77	26.64	0.76	2.99	FA/FOP-28	28.25	45.60	0.81	6.96
FA/COP-12	12.31	29.70	0.77	3.00	CA/FOP-0	0	0.00	3.05	5.94
FA/COP-14	13.86	32.62	0.84	3.01	CA/FOP-2	2.17	4.75	3.21	5.19
FA/COP-15	15.31	35.23	0.93	3.31	CA/FOP-4	4.06	8.69	3.21	4.92
FA/COP-17	16.73	37.68	0.86	3.94	CA/FOP-6	6.01	12.57	3.24	5.18
FA/COP-18	18.1	39.94	0.95	4.23	CA/FOP-8	8.05	16.44	3.55	5.94
CA/COP-0	0	0.00	2.96	5.94	CA/FOP12	11.5	22.61	4.15	4.92
CA/COP-2	2.01	6.12	3.07	4.53	CA/FOP-14	14.29	27.26	5.63	5.19
CA/COP-4	4.09	11.93	3.09	4.53	CA/FOP-18	18.8	34.23	5.23	6.17
CA/COP-6	6.08	17.06	3.1	4.82	CA/FOP-22	22.36	39.30	6.37	6.52
CA/OP-8	8.05	21.76	3.24	5.53	CA/FOP-24	24.05	41.58	7.38	7.70
CA/COP-10	10.15	26.41	3.29	5.38	FSS/TP-0	0	0.00	1.99	2.85
CA/COP-12	12.24	30.70	3.38	5.58	FSS/TP-1	1	13.20	2.14	6.43
FA/COP-14	14.31	34.66	3.49	5.58	FSS/TP-2	2	23.50	3.65	6.45
CA/COP-16	16.36	38.33	3.42	6.10	FSS/TP-3	3.5	35.31	8.22	9.84
UFA/FOP-0	0	0.00	0.35	1.04	FSS/TP-5	5.2	45.22	8.48	10.69
UFA/FOP-2	2.17	4.43	0.34	4.12	FSS/TP-9	9	59.81	12.33	12.74
UFA/FOP-4	4.13	8.26	0.34	4.28	CSS/TP-0	0	0.00	3.75	6.43
UFA/FOP-6	6.06	11.88	0.35	3.84	CSS/TP-1	1	12.92	6.1	8.00
UFA/FOP-8	8.05	15.47	0.36	4.13	CSS/TP-2	2	23.06	8.3	9.50
UFA/FOP-10	10.16	19.12	0.38	4.27	CSS/TP-3	3.5	34.75	10.7	11.30
UFA/FOP-12	12.04	22.25	0.28	4.41	FA/TP-1	1	7.37	0.87	2.69
UFA/FOP-14	14.06	25.49	0.38	5.67	FA/TP-2	2	13.84	0.92	2.69
UFA/FOP-16	16.26	28.87	0.37	5.33	FA/TP-3	3	19.58	1.15	3.01

Table 3
MAPE of U_{mf} and U_{cf} obtained by CCA as function of different set of inputs.

# of test	Inert			Biomass				%Biomass		MAPE, %	
	ρ^I_{bulk}	ρ^I_{part}	d^I_{Sauter}	ρ^B_{bulk}	ρ^B_{part}	L_B	Φ_B	%w	%vol	U_{mf}	U_{cf}
1	–	×	×	–	×	×	×	×	–	65.54	20.31
2	–	×	×	–	×	×	×	–	×	76.02	17.98
3	×	×	×	×	×	×	×	×	–	65.53	20.24
4	×	×	×	×	×	×	×	–	×	75.98	18.18
5	–	×	×	–	×	×	×	×	×	40.72	17.52

in mass for tests 1 and 3, and in volume for tests 2 and 4, in order to evaluate which of the 2 variables has a positive effect on the performance of the statistical analysis. Finally, for the test 5 the effect of the biomass fraction in the bed was considered both by weight and by volume.

In general, the CCA shows poor performance for U_{mf}: a positive effect occurs when the biomass fraction (%wt.) in the bed is present among the inputs (tests 1 and 3), on the contrary the biomass fraction in the bed by volume tends to have a negative effect (test 2 and 4). However, a substantial improvement, even if the MAPE remains very high (greater than 40%), occurs when both biomass fractions are used as inputs. The main difficulty of the CCA is found for low U_{mf} values (<1cm/s), which mainly concerns mixtures where the inert is alumina below 150 μm. Probably this is related to the fact that the inert belongs to Geldart A particle classification, which includes particles exhibiting a non-uniform fluidization regime.

Conversely, the performances on U_{cf} were much better, even if the effect of the biomass fraction is opposite with respect to that found for U_{mf}. Actually, the best results were obtained when the volume value was used (tests 2 and 4), obtaining MAPEs of approximately 18%; instead, the utilization of the weight fraction triggers an increase in the error of about 2 % points (tests 1 and 3). The presence of both fractions improves performance slightly (test 5). In conclusion, the best performance of CCA were MAPE values of 40.72% for U_{mf} and 17.52% for U_{cf}.

The set of inputs used for the training of the ANNs, the same for U_{mf} and U_{cf}, are those referred to the test 2 of the CCA. This choice was made because it gives the best combination between the number of inputs used and the value of the MAPE on U_{cf}, which is the variable of greatest interest here. Fig. 5 shows the MAPE values resulting from the training of the three different networks with different architecture as a function of the number of neurons.[1] The training function was also varied for each type of network and number of neurons, thus testing 12 different types, for a total of 216 + 216 neural networks trained for U_{mf} and U_{cf}. However, for the sake of clarity, only the best network obtained from the 12 different types of training functions is reported for each value of the number of neurons.

Unlike the CCA, the ANNs perform better on U_{mf} than on U_{cf}, even if in general it occurs that the ANNs have much better performances than the statistical analysis. For U_{mf} the best network was the fitnet with 7 neurons (training function based on Bayesian Regularization algorithm) with a MAPE value of about 4%.

Both the fitnet and the feedforward have a very similar trend unlike the cascadeforwardnet, which instead differs greatly from the other two, in particular, for intermediate values of the number of neurons (Fig. 5 on the left). The differences among the type on ANN becomes less evident for U_{cf} (Fig. 5 on the right). For U_{cf} the best ANN was the feedforward net with 6 neurons and, as in this case of Umf, the best training function was the Bayesian Regularization algorithm. The MAPE obtained was about 6.71%. The best ANNs for the two outputs were further explored in detail in order to assess the impact of individual inputs on individual outputs.[2] Fig. 6 compares the real values of U_{mf} and U_{cf} with those expected (U^*_{mf} and U^*_{cf}) from the respective ANN networks. For U_{mf} it is possible to note that, also for low values, a satisfactory prediction is granted by the model, unlike the CCA, with a R^2 of 0.98. This demonstrates the great ability of ANN to manage complex relationships among physical properties. Also, for U_{cf} the accordance with U^*_{cf} was very good, presenting a $R^2 = 0.93$. The application of the connection weight method [32–34] has permitted to evaluate the impact of individual inputs on the machine learning process (Table 4). For U_{mf}, the particle density of the inert has the greatest impact of approximately 46%, followed by the sphericity (23.8%) and the characteristic size of the biomass (11.8%). The strong impact of the particle density of the inert is almost certainly due to the fact that, when the minimum fluidization condition is reached, only the inert material begins to fluidize, while the biomass remains static in segregated conditions. U_{cf} is strongly dependent both on the particle density of the inert (31.4%) and on the volumetric fraction of the biomass in the bed (31.9%), as expected, and on the particle density of the biomass itself (13.6%), albeit to a lesser extent. Vice versa, the characteristic size and sphericity of the biomass seem to play a marginal role; this result was certainly not predictable and would deserve further investigation.

4. Conclusions

Evidence from literature shows that currently available correlations to predict the minimum fluidization velocity of binary mixtures including biomass exhibit significant limitations in terms of accuracy and/or applicability, being appropriate only for specific binary mixture types. Further work is, therefore, needed to develop more accurate and generic correlations as well as to provide additional insight on predicting the fluidization behavior of biomass-based binary mixtures, which are encountered in many industrial processes spanning the manufacture of energy, material and resources to greenhouse emissions mitigation and renewable resources utilization.

In this context, the present work investigated the fluidization and segregation behaviour of poly-disperse binary mixtures of biomass and inert particles. In particular, air-dried orange and tomato peels were used as biomass feedstock while several granular solids with the same density but different size or with the same size but different density were tested as inert bed component in order to determine the prevalence of the effect of either size or density on the fluidization and segregation behavior of the investigated binary systems. Tests at different weight fraction of the biomass in the bed were also performed for each of the investigated binary systems. Results suggest that the bed components' density difference prevails over the size difference in determining the mixing/segregation behavior of binary fluidized bed, whereas the velocities of minimum and complete fluidization increased with the increase of the biomass weight fraction in the bed. The results from the experimental campaign have been used to create the dataset for the

[1] The comparison of MAPE behaviour with the number of neurons with MAE, MSA and SAE is included in the supplementary material.

[2] Weights and bias matrices for the best ANNs are reported in the supplementary materials.

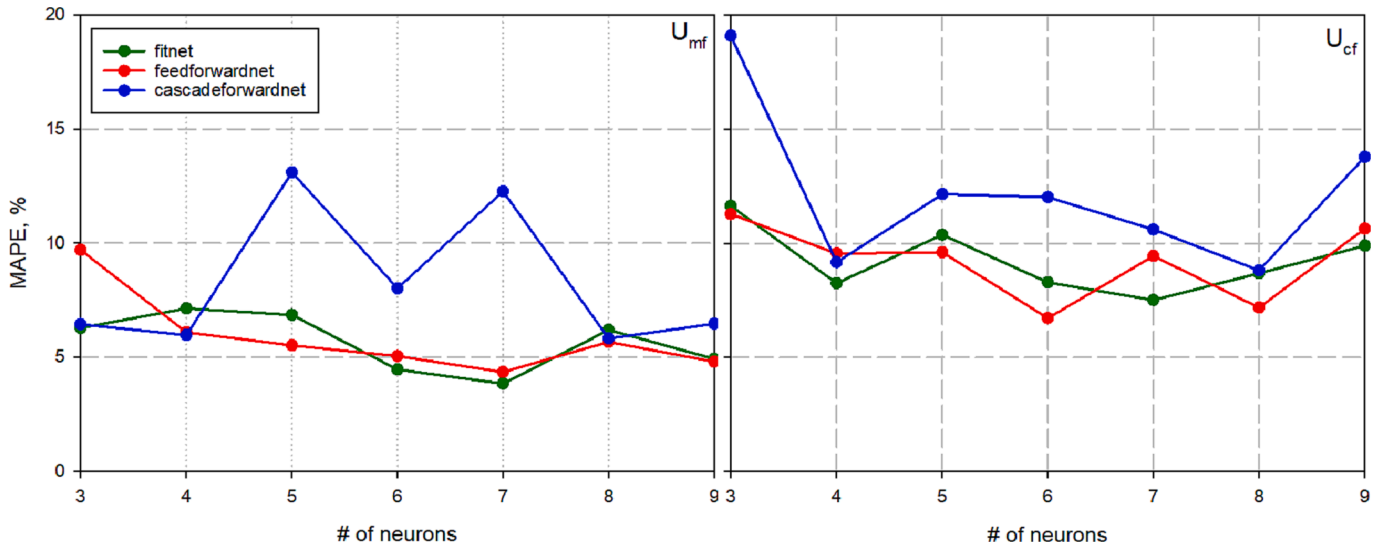

Fig. 5. MAPE obtained by the training of the three different networks as function of the number of neurons. U_{mf} of the left and U_{cf} on the right.

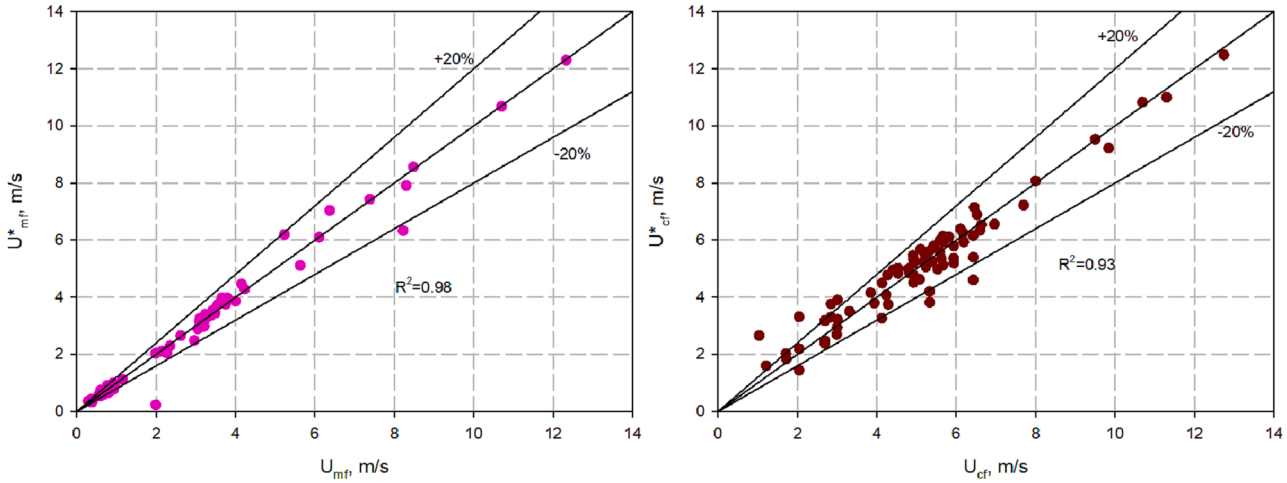

Fig. 6. Comparison of the experimental results and predicted results derived from the ANN. U_{mf} of the left and U_{cf} on the right.

Table 4
Relative importance of different inputs on U_{mf} and U_{cf}.

Variable	ρ^{I}_{part}	d^{I}_{Sauter}	ρ^{B}_{part}	L_B	Φ_B	%volBiomass
U_{mf}	46.8%	2.5%	3.8%	11.8%	23.8%	11.3%
U_{cf}	31.4%	9.4%	13.6%	6.9%	6.8%	31.9%

training of ANNs in MATLAB environment for predictions of U_{mf} and U_{cf} of binary mixtures. Before the developing of ANNs, also a multivariate statistical analysis has been developed by the implementation of Canonical Correlation Analysis (CCA). The results from CCA showed poor performance in terms of prediction for U_{mf}, where main fails have been observed for fine inert materials belonging to Geldart A group. Conversely, ANNs demonstrated good performances for both outputs (U_{mf} and U_{cf}), moreover, in opposite to CCA, best predictions have been obtained for U_{mf} with a MAPE $< 4\%$ ($R^2 = 0.98$), while for U_{cf} the best ANN returned a MAPE of about 7% ($R^2 = 0.93$). The analysis on the relative importance of the different outputs showed interesting results, which deserve a deeper investigation. Indeed, U_{mf} depends strongly, as expected, on particle density of the inert and on the sphericity of the biomass, but the volumetric percentage of the biomass in the mixture and its characteristic length have had a lower impact on the results. This may be due to the fact, that at minimum fluidization conditions only the inert fluidizes, while the biomass remains static and segregated, and probably its presence in the bed represents, in a certain way, an obstacle to the movement of the inert. Conversely, the volumetric fraction of the biomass in the mixture becomes relevant for the prediction of U_{cf}, while the sphericity and the characteristic length of the biomass have a marginal role, as if the morphological characteristics of biomass become less important in conditions of complete fluidization of the bed. However, this work represents only a first attempt for applying machine learning techniques for such problems, and more in-depth analysis will be faced in the future including the use of other techniques such as Regression tree, Random Forest, or Support Vector Machine method.

CRediT authorship contribution statement

Vincenzo Del Duca: Data curation, Formal analysis, Investigation, Software, Writing – original draft. **Paola Brachi:** Methodology, Investigation, Resources, Project administration, Software, Writing – original draft, Conceptualization. **Riccardo Chirone:** Writing – original draft. **Roberto Chirone:** Formal analysis, Supervision, Validation, Visualization, Writing – original draft. **Antonio Coppola:** Formal analysis, Methodology, Resources, Project administration, Software, Writing – original draft, Conceptualization. **Michele Miccio:** Supervision,

Validation, Writing – original draft. **Giovanna Ruoppolo:** Supervision, Visualization, Writing – original draft.

Declaration of Competing Interest

The authors declare that they have no known competing financial interests or personal relationships that could have appeared to influence the work reported in this paper.

Data availability

Data will be made available on request.

Appendix A. Supplementary data

Supplementary data to this article can be found online at https://doi.org/10.1016/j.fuel.2023.128314.

References

[1] Iannello S, Morrin S, Materazzi M. Fluidised bed reactors for the thermochemical conversion of biomass and waste. KONA Powder Part J 2020;37:114–31. https://doi.org/10.14356/kona.2020016.

[2] Pérez NP, Pedroso DT, Machin EB, Antunes JS, Verdú Ramos RA, Silveira JL. Fluid dynamic study of mixtures of sugarcane bagasse and sand particles: Minimum fluidization velocity. Biomass Bioenergy 2017;107:135–49. https://doi.org/10.1016/j.biombioe.2017.08.015.

[3] Cáceres-Martínez LE, Guío-Pérez DC, Rincón-Prat SL. Significance of the particle physical properties and the Geldart group in the use of correlations for the prediction of minimum fluidization velocity of biomass–sand binary mixtures. Biomass Convers Biorefinery 2023;13:935–51. https://doi.org/10.1007/s13399-020-01189-9.

[4] Fu Z, Zhu J, Barghi S, Zhao Y, Luo Z, Duan C. Minimum fluidization velocity of binary mixtures of medium particles in the Air Dense medium fluidized bed. Chem Eng Sci 2019;207:194–201. https://doi.org/10.1016/j.ces.2019.06.005.

[5] Anantharaman A, Cocco RA, Chew JW. Evaluation of correlations for minimum fluidization velocity (Umf) in gas-solid fluidization. Powder Technol 2018;323:454–85. https://doi.org/10.1016/j.powtec.2017.10.016.

[6] Alghamdi YA, Peng Z, Almutairi Z, Alibrahim H, Al-Alweet FM, Moghtaderi B, et al. Assessment of correlations for minimum fluidization velocity of binary mixtures of particles in gas fluidized beds. Powder Technol 2021;394:1231–9.

[7] Himmelblau DM. Accounts of experiences in the application of artificial neural networks in chemical engineering. Ind Eng Chem Res 2008;47:5782–96. https://doi.org/10.1021/ie800076s.

[8] Chew JW, Cocco RA. Application of machine learning methods to understand and predict circulating fluidized bed riser flow characteristics. Chem Eng Sci 2020;217:115503. https://doi.org/10.1016/j.ces.2020.115503.

[9] Chew JW, Cocco RA. Do particle-related parameters influence circulating fluidized bed (CFB) riser flux and elutriation? Chem Eng Sci 2020;227:115935. https://doi.org/10.1016/j.ces.2020.115935.

[10] Fu Y, Wang S, Xu X, Zhao Y, Dong L, Chen Z. Particle flow characteristics in a gas-solid separation fluidized bed based on machine learning. Fuel 2022;314:123039. https://doi.org/10.1016/j.fuel.2021.123039.

[11] Rushd S, Parvez MT, Al-Faiad MA, Islam MM. Towards optimal machine learning model for terminal settling velocity. Powder Technol 2021;387:95–107. https://doi.org/10.1016/j.powtec.2021.04.011.

[12] Zhong W, Chen X, Grace JR, Epstein N, Jin B. Intelligent prediction of minimum spouting velocity of spouted bed by back propagation neural network. Powder Technol 2013;247:197–203. https://doi.org/10.1016/j.powtec.2013.07.022.

[13] Saldarriaga JF, Freire F, Freire J. Adjustment of the minimum spouting velocity in a conical spouted bed from artificial neural networks. Chem Eng Trans 2018;70:1243–8. https://doi.org/10.3303/CET1870208.

[14] Targino TG, Freire JT, Perazzini MTB, Perazzini H. Fluidization design parameters of agroindustrial residues for biomass applications: experimental, theoretical, and neural networks approach. Biomass Convers Biorefinery 2023;13(5):4213–28.

[15] Zhou J, Liu D, Ye M, Liu Z. Data-Driven Prediction of Minimum Fluidization Velocity in Gas-Fluidized Beds Using Data Extracted by Text Mining. Ind Eng Chem Res 2021;60:13727–39. https://doi.org/10.1021/acs.iecr.1c02307.

[16] Souto BA, Souza VLC, Bitti Perazzini MT, Perazzini H. Valorization of acai bio-residue as biomass for bioenergy: Determination of effective thermal conductivity by experimental approach, empirical correlations and artificial neural networks. J Clean Prod 2021:279. https://doi.org/10.1016/j.jclepro.2020.123484.

[17] Perazzini H, Perazzini MTB, Meili L, Freire FB, Freire JT. Artificial neural networks to model kinetics and energy efficiency in fixed, fluidized and vibro-fluidized bed dryers towards process optimization. Chem Eng Process - Process Intensif 2020;156:108089. https://doi.org/10.1016/j.cep.2020.108089.

[18] Brachi P, Chirone R, Miccio F, Miccio M, Ruoppolo G. Valorization of Orange Peel Residues via Fluidized Bed Torrefaction: Comparison between Different Bed Materials. Combust Sci Technol 2019;191:1585–99. https://doi.org/10.1080/00102202.2019.1582526.

[19] Midhun Prasad K, Murugavelh S. Experimental investigation and kinetics of tomato peel pyrolysis: Performance, combustion and emission characteristics of bio-oil blends in diesel engine. J Clean Prod 2020;254:120115. https://doi.org/10.1016/j.jclepro.2020.120115.

[20] Bruni G, Solimene R, Marzocchella A, Salatino P, Yates JG, Lettieri P, et al. Self-segregation of high-volatile fuel particles during devolatilization in a fluidized bed reactor. Powder Technology 2002;128(1):11–21.

[21] Brachi P, Chirone R, Miccio F, Miccio M, Ruoppolo G. Segregation and fluidization behavior of poly-disperse mixtures of biomass and inert particles. Chem Eng Trans 2017;57:811–6. https://doi.org/10.3303/CET1757136.

[22] Agu CE, Ugwu A, Pfeifer C, Eikeland M, Tokheim LA, Moldestad BME. Investigation of Bubbling Behavior in Deep Fluidized Beds at Different Gas Velocities using Electrical Capacitance Tomography. Ind Eng Chem Res 2019;58:2084–98. https://doi.org/10.1021/acs.iecr.8b05013.

[23] Zhang Y, Jin B, Zhong W. Experimental investigation on mixing and segregation behavior of biomass particle in fluidized bed. Chem Eng Process Process Intensif 2009;48:745–54. https://doi.org/10.1016/j.cep.2008.09.004.

[24] Clarke KL, Pugsley T, Hill GA. Fluidization of moist sawdust in binary particle systems in a gas-solid fluidized bed. Chem Eng Sci 2005;60:6909–18. https://doi.org/10.1016/j.ces.2005.06.004.

[25] Formisani B, Girimonte R, Longo T. The fluidization process of binary mixtures of solids: Development of the approach based on the fluidization velocity interval. Powder Technol 2008;185:97–108. https://doi.org/10.1016/j.powtec.2007.10.003.

[26] Formisani B, Girimonte R. Experimental analysis of the fluidization process of binary mixtures of solids. KONA Powder Part J 2003;21:66–75. https://doi.org/10.14356/kona.2003010.

[27] Zhang Y, Jin B, Zhong W. Fluidization, mixing and segregation of a biomass-sand mixture in a fluidized bed. Int J Chem React Eng 2008:6. https://doi.org/10.2202/1542-6580.1809.

[28] Marzocchella A, Salatino P, Di Pastena V, Lirer L. Transient fluidization and segregation of binary mixtures of particles. AIChE J 2000;46:2175–82. https://doi.org/10.1002/aic.690461110.

[29] Kunii D, Levenspiel O. Fluidization engineering. Butterworth-Heinemann; 1991.

[30] Yang W. Handbook of fluidization and fluid-particle systems. CRC Press; 2003.

[31] Hsieh WW. Nonlinear canonical correlation analysis by neural networks. Neural Netw 2000;13:1095–105. https://doi.org/10.1016/S0893-6080(00)00067-8.

[32] Olden JD, Jackson DA. Illuminating the "black box": Understanding variable contributions in artificial neural networks. Ecol Modell 2002;154:135–50.

[33] Olden JD, Joy MK, Death RG. An accurate comparison of methods for quantifying variable importance in artificial neural networks using simulated data. Ecol Modell 2004;178:389–97. https://doi.org/10.1016/j.ecolmodel.2004.03.013.

[34] Gevrey M, Dimopoulos I, Lek S. Review and comparison of methods to study the contribution of variables in artificial neural network models. Ecol Modell 2003;160:249–64. https://doi.org/10.1016/S0304-3800(02)00257-0.